ISSN : 0974 - 7435 Volume 10 Issue 23

2014

BioTechnology

An Indian Journal

FULL PAPER

BTAIJ, 10(23), 2014 [14432-14440]

The application of adaptive internal model control in large-capacity synchronous motor vector control system

Xie Lun[1*], Wang Ya-Meng[2], Hu Bo[1], Wang Zhi-Liang[1], Sun Tie[2]

[1]School of Computer and Communication Engineering, University of Science and Technology Beijing, Beijing, 100083, (CHINA)

[2]School of Automation and Electrical Engineering, University of Science and Technology Beijing, Beijing, 100083, (CHINA)

E-mail: xielun@ustb.edu.cn

ABSTRACT

In the air gap flux-oriented vector control system, which is built based on the AC-DC-AC variable frequency speed control equipment of the large capacity synchronous motor, there are many problems, such as DC bias and dependence on motor parameters existing in the traditional voltage model flux observer. In addition, the pure integral element in the voltage model caused problems such as DC bias and integral saturation. Overcoming these problems will improve the observation accuracy of the flux and get good dynamic performance and robustness at the same time. Aimed at the above-mentioned problems, an improved voltage model flux observer based on adaptive internal model control is proposed. In consideration of the disturbance canceling structure in the adaptive inverse control system, the disturbance canceling model is built in this control system. At last, the cascaded LPF with compensation structure is set up to improve the model. The simulation research has been done by applying the improved voltage model in the 2500kw synchronous motor vector control system. The experimental results showed that the enhanced voltage model can prohibit the impact caused by the pure integral element, the parametric variation and the disturbance. The flux observation precision is increased by more than 10 times.

KEYWORDS

Large capacity synchronous motor; AC-DC-AC variable frequency; Voltage model; Adaptive internal model control; Disturbance canceling.

INTRODUCTION

Because of AC synchronous motor's large overload capacity, high power factor and efficiency, it's widely used in high-power low-speed production machinery, such as rolling mill, mine hoist, etc.

In the air-gap flux-oriented vector control theory, Mu unit's function in voltage model flux observer is to identify the flux of synchronous motor, stator resistance and stator leakage inductance. It may affect control accuracy. In actual control, because motor changes with operating conditions, for instance, motor load and load rejection process, the motor parameters will exist perturbation. Besides, external uncertain disturbance factors still can't be ignored. In this case, traditional voltage model over-relied on parameters result in low accuracy and poor robustness. There are two mature methods including internal model control [1] and model reference adaptive control. Converging the two methods, the adaptive internal model controller (AIMC) [2] for synchronous motor voltage model is established. In recent years, scholars proposed extensive research and made lots of improvements in algorithm. Like this, accurate mathematical model's structure does not too much depend on controlled object with good track performance and resisting ability of outside interference. It is widely used in process control and motor control [3,4]. In consideration of the disturbance canceling structure in the adaptive inverse control system, the disturbance canceling model is built. It guaranteed the robustness of the system without sacrificing tracking performance. This paper applied the improved model to a large-capacity synchronous motor AC-DC-AC variable frequency vector control system, and then simulated in the AC-DC-AC variable frequency vector control system, which is built on the PSIM. Then we got the simulation results of the control system under typical conditions.

DESIGN OF VOLTAGE MODEL FLUX OBSERVER

AC synchronous motor voltage model

The voltage model equation of synchronous motor under AC synchronous motor air gap flux oriented control can be expressed as follow:

$$\begin{cases} \psi_{\delta\alpha} = \int E_\alpha dt = \int (u_{s\alpha} - R_s i_{s\alpha})dt - L_{sl} i_{s\alpha} \\ \psi_{\delta\beta} = \int E_\beta dt = \int (u_{s\beta} - R_s i_{s\beta})dt - L_{sl} i_{s\beta} \end{cases} \quad (1)$$

Where: $u_{s\alpha}$, $u_{s\beta}$ were defined as $\alpha\beta$ axis component of the stator voltage respectively, $i_{s\alpha}$, $i_{s\beta}$ were defined as $\alpha\beta$ axis component of the stator current respectively, R_s was defined as stator resistance, L_{sl} was defined as stator winding leakage inductance coefficient, $\psi_{\delta\alpha}$, $\psi_{\delta\beta}$ were defined as $\alpha\beta$ axis component of flux respectively.

Design of voltage model internal model controller

As a unique control system structure, internal model control (IMC) originated in the process control, and was successfully applied [5]. The design idea is parallel the object model and actual object, and the controller approximate model's dynamic inversion. In the design of internal model controller, we need precise controlled object mathematical model. When the model matched well, in the way of internal model controller's designation, we got satisfactory control effect [6].

Mu unit in stator voltage model, we calculated the flux based on the stationary coordinate $\alpha\beta$ axis voltage and current, input stator voltage and current, output $\alpha\beta$ axis flux, $\psi_{s\alpha}$, $\psi_{s\beta}$, then obtained the flux amplitude $|\psi_s|$ and θ angle between M axis and α axis. By using Laplace transform, formula (1) can be deformed into:

$$\begin{cases} E_a(s) = u_{s\alpha}(s) - (R_s + sL_{sl}) i_{s\alpha}(s) \\ E_\beta(s) = u_{s\beta}(s) - (R_s + sL_{sl}) i_{s\beta}(s) \end{cases} \quad (2)$$

We defined $E'_\alpha = E_\alpha - u_{s\alpha}$, $E'_\beta = E_\beta - u_{s\beta}$, according to the internal model theory, we made the following deformation, the given value $R(s) = \begin{bmatrix} i^*_{s\alpha} \\ i^*_{s\beta} \end{bmatrix}$, we can compute:

$$Y(s) = G(s)U(s) \quad (3)$$

Where $G(s) = \begin{bmatrix} -R_s - sL_{sl} & 0 \\ 0 & -R_s - sL_{sl} \end{bmatrix}^{-1}$,

$$Y(s)=\begin{bmatrix} i_{s\alpha}(s) \\ i_{s\beta}(s) \end{bmatrix}, \quad U(s)=\begin{bmatrix} E'_{\alpha}(s) \\ E'_{\beta}(s) \end{bmatrix},$$

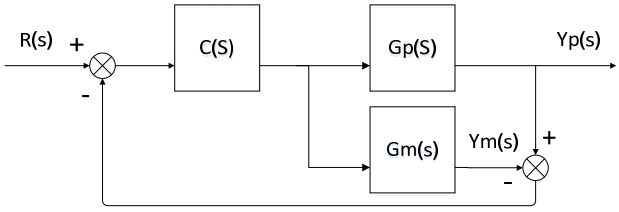

Figure 1: The structure of the voltage model with IMC

$C(s)=G_m^{-1}(s)Q(s)=G_p^{-1}(s)Q(s)$, $Q(s)$ was feed-forward low pass filter, as there is no zero point in right half plane, system is stable and can be approximated as a first-order system, we can select $Q(s)=\dfrac{\alpha}{s+\alpha}I$, where α is adjustable coefficient, we obtained:

$$C(s)=G_p^{-1}(s)Q(s)=\begin{bmatrix} -R_s-sL_{sl} & 0 \\ 0 & -R_s-sL_{sl} \end{bmatrix}Q(s) \qquad (4)$$

Adaptive internal model controller

IMC voltage model performance depends on the match situation of prediction internal model and actual motor model. When controlled object model is unknown or parameters change slowly over time, there is no priori model for the controller's designation [7]. Here, we must identify model's parameters online by online identification technology, and correct IMC voltage model in time. When the controlled object reference model and the actual model mismatched seriously, the quality of control system will deteriorate. So, it's an important part for this paper to improve the robustness of the control system by adaptive ability. In this paper, we designed the voltage model [8] by combining internal model control with model reference adaptive control. Combined with the idea of internal model control thought, we deduced the reference model adaptive rule, so that the controller parameters were adjusted automatically.

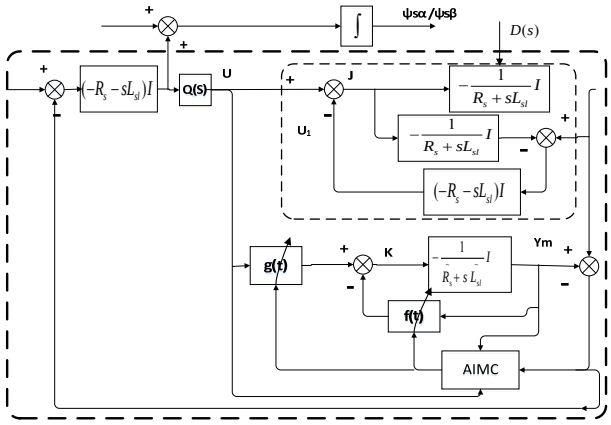

Figure 2: The structure of the voltage model with AIMC

Disturbance canceling structure

In this paper, we introduced the disturbance canceling structure widely used in the adaptive inverse control system [9], so that both dynamic response of object and disturbance control can achieve optimal without compromise. We built disturbance canceling structure in the voltage model adaptive internal model control system, the object input drove both the object and the model (There is no noise and disturbance in the model), use the bias between the object and model as inverse model's inputs. Calculate the system's disturbance and minus it in the actual inputs, then we eliminated the disturbance [10]. In Figure 2, the small dashed box stands for the disturbance elimination model.

According to the mathematical model of the voltage model mentioned before. We can assume the transfer function of controlled object in voltage model as follows:

$$G_p(s)=G_{p0}(s)=\begin{bmatrix}-R_s-sL_{sl} & 0\\ 0 & -R_s-sL_{sl}\end{bmatrix}^{-1}$$

Inverse function: $G_n(s)=\begin{bmatrix}-R_s-sL_{sl} & 0\\ 0 & -R_s-sL_{sl}\end{bmatrix}$

The control object satisfies the equation:

$$Y_P(s)=J(s)G_p(s)-D(s)G_p(s)$$

The control object model satisfies the equation:

$$Y_{P0}(s)=J(s)G_{p0}(s)$$

The control object and control model's deviation satisfy the equation:

$$\epsilon(s)=Y_p(s)-Y_{p0}(s)=-D(s)G_p(s)$$

So we can deduce:

$$U_1(s)=G_n(s)\epsilon(s)=-D(s)$$

$$M(s)=U(s)-U_1(s)=U(s)+D(s)$$

The control object equation was converted into the following form:

$$Y_p(s)=(U(s)+D(s))G_p(s)-D(s)G_p(s)=U(s)G_p(s) \quad (5)$$

We can eliminate the disturbance by this structure.

Adaptive internal model structure

In Figure 2, the bigger dashed box stands for the adaptive internal model control (AIMC) model.

Differential equations for the control object:

$$\dot{y}_p(t)=Ay_p(t)+Bu(t)$$

Where: $A=\begin{bmatrix}-\frac{R_s}{L_{sl}} & 0\\ 0 & -\frac{R_s}{L_{sl}}\end{bmatrix}, B=\begin{bmatrix}-\frac{1}{L_{sl}} & 0\\ 0 & -\frac{1}{L_{sl}}\end{bmatrix},$

$$y_p(t)=\begin{pmatrix}i_{s\alpha}\\ i_{s\beta}\end{pmatrix}, u(t)=\begin{pmatrix}E'_{\alpha}\\ E'_{\beta}\end{pmatrix}$$

Differential equations for the reference model:

$$\dot{y}_m(t)=\tilde{A}y_m(t)+\tilde{B}k(t)$$

Add feedforward-feedback control to the model [11,12], we deduced reference model input:

$$k(t)=g(t)u(t)-f(t)y_m(t)$$

Where $g(t)$ and $f(t)$ were defined as adaptive adjustable parameters respectively.

We can obtain:

$$\dot{y}_m(t)=\tilde{A}y_m(t)+\tilde{B}\left(g(t)u(t)-f(t)y_m(t)\right)=\left(\tilde{A}-\tilde{B}f(t)\right)y_m(t)+\tilde{B}g(t)u(t) \quad (6)$$

Where: $\tilde{A}=\begin{bmatrix}-\frac{\tilde{R}_s}{\tilde{L}_{sl}} & 0\\ 0 & -\frac{\tilde{R}_s}{\tilde{L}_{sl}}\end{bmatrix}, \tilde{B}=\begin{bmatrix}-\frac{1}{\tilde{L}_{sl}} & 0\\ 0 & -\frac{1}{\tilde{L}_{sl}}\end{bmatrix},$

$$y_m(t)=\begin{pmatrix}\tilde{i}_{s\alpha}\\ \tilde{i}_{s\beta}\end{pmatrix}, u(t)=\begin{pmatrix}E'_{\alpha}\\ E'_{\beta}\end{pmatrix}$$

We define error: $e(t)=y_p(t)-y_m(t)$

We can obtain:

$$\dot{e}(t)=\dot{y}_p(t)-\dot{y}_m(t)=Ae(t)+My_m(t)+Nu(t) \quad (7)$$

Where:

$$M = A - \tilde{A} + \tilde{B}f(t)$$

$$= \begin{pmatrix} -\frac{R_s}{L_{sl}} + \frac{\tilde{R}_s}{\tilde{L}_{sl}} & 0 \\ 0 & -\frac{R_s}{L_{sl}} + \frac{\tilde{R}_s}{\tilde{L}_{sl}} \end{pmatrix} + \begin{bmatrix} \frac{-1}{\tilde{L}_{sl}} & 0 \\ 0 & -\frac{1}{\tilde{L}_{sl}} \end{bmatrix} f(t)$$

$$N = B - \tilde{B}g(t)$$

$$= \begin{pmatrix} -\frac{1}{L_{sl}} & 0 \\ 0 & -\frac{1}{L_{sl}} \end{pmatrix} + \begin{pmatrix} \frac{1}{\tilde{L}_{sl}} & 0 \\ 0 & \frac{1}{\tilde{L}_{sl}} \end{pmatrix} g(t)$$

Formula (7) was transformed as follow:

$$\dot{e}(t) == Ae(t) + \phi^{\mathrm{T}}\tau$$

Where: $\phi^{\mathrm{T}} = \begin{pmatrix} M & N \end{pmatrix}$, $\tau = \begin{pmatrix} y_m(t) & u(t) \end{pmatrix}^{\mathrm{T}}$

The Lyapunov function was designed based on the Lyapunov stability theorem [13]:

$$V(y,t) = \frac{1}{2}\left(e^{\mathrm{T}}Pe + \frac{1}{\lambda}\phi^{\mathrm{T}}Q\phi \right) \tag{8}$$

In order to ensure the rule above matrix positive definite, we define P,Q as unit arrays, $\lambda > 0$, set a stable equilibrium point $e = \phi^{\mathrm{T}} = 0$,differentiate the formula (8):

$$\dot{V}(y,t) = \frac{1}{2}\left(\dot{e}^{\mathrm{T}}Pe + e^{\mathrm{T}}P\dot{e} + \frac{1}{\lambda}\dot{\phi}^{\mathrm{T}}Q\phi + \frac{1}{\lambda}\phi^{\mathrm{T}}Q\dot{\phi} \right)$$

$$= \frac{1}{2}(e^{\mathrm{T}}A^{\mathrm{T}}Pe + \tau^{\mathrm{T}}\phi Pe + e^{\mathrm{T}}PAe + e^{\mathrm{T}}P\phi^{\mathrm{T}}\tau + \frac{1}{\lambda}\dot{\phi}^{\mathrm{T}}Q\phi + \frac{1}{\lambda}\phi^{\mathrm{T}}Q\dot{\phi}) \tag{9}$$

$$= \frac{1}{2}e^{\mathrm{T}}(A^{\mathrm{T}}P + PA)e + \frac{1}{2}(\tau^{\mathrm{T}}\phi Pe + e^{\mathrm{T}}P\phi^{\mathrm{T}}\tau + \frac{1}{\lambda}\dot{\phi}^{\mathrm{T}}Q\phi + \frac{1}{\lambda}\phi^{\mathrm{T}}Q\dot{\phi})$$

And $A^{\mathrm{T}}P + PA = \begin{pmatrix} -\frac{2R_s}{L_{sl}} & 0 \\ 0 & -\frac{2R_s}{L_{sl}} \end{pmatrix}$, so the first item of formula is negative, if guarantee the sum of the last two items is zero, we can satisfy $\dot{V}(y,t)$ is negative.

So we can deduce:

$$\frac{1}{2}(\tau^{\mathrm{T}}\phi Pe + e^{\mathrm{T}}P\phi^{\mathrm{T}}\tau + \frac{1}{\lambda}\dot{\phi}^{\mathrm{T}}Q\phi + \frac{1}{\lambda}\phi^{\mathrm{T}}Q\dot{\phi}) = 0 \tag{10}$$

By the calculation:

$$\tau^{\mathrm{T}}\phi Pe = e^{\mathrm{T}}P\phi^{\mathrm{T}}\tau = (y_m{}^{\mathrm{T}}M + u^{\mathrm{T}}N)e$$

$$\dot{\phi}^{\mathrm{T}}Q\phi = \phi^{\mathrm{T}}Q\dot{\phi} = \dot{M}M + \dot{N}N$$

The formula (10) can be transformed as follow:

$$(y_m{}^{\mathrm{T}}M + u^{\mathrm{T}}N)e + \frac{1}{\lambda}(\dot{M}M + \dot{N}N) = 0$$

That is: $\begin{cases} (y_m{}^{\mathrm{T}}e + \frac{1}{\lambda}\dot{M})M = 0 \\ (u^{\mathrm{T}}e + \frac{1}{\lambda}\dot{N})N = 0 \end{cases}$

So we can deduce: $\begin{cases} \dot{M} = -\lambda y_m{}^{\mathrm{T}}e \\ \dot{N} = -\lambda u^{\mathrm{T}}e \end{cases}$

And: $\begin{cases} \dot{M} = \bar{B}\bar{f}(t) \\ \dot{N} = -\bar{B}\bar{g}(t) \end{cases}$

We can obtain: $\begin{cases} \bar{f}(t) = -Iy_m^{\mathrm{T}}e \\ \bar{g}(t) = Iu^{\mathrm{T}}e \end{cases}$, where $I = \frac{\lambda}{\bar{B}}$

Now, Lyapunov function satisfies $V(t) > 0$, $\dot{V}(t) < 0$, so the whole system is wide range global stable at equilibrium point [14].

Cascaded low pass filter(LPF) with compensation structure

As the pure integral element in the voltage model caused DC bias and integral saturation, the flux waveforms occurred serious deviation [15], the error is serious, it's an urgent problem need to be solved. This paper presented an improved voltage model, the voltage and current were processed respectively, at last, compensate amplitude and phase [16]. In Figure 3, the dashed box stands for the cascaded low pass filter with compensation structure.

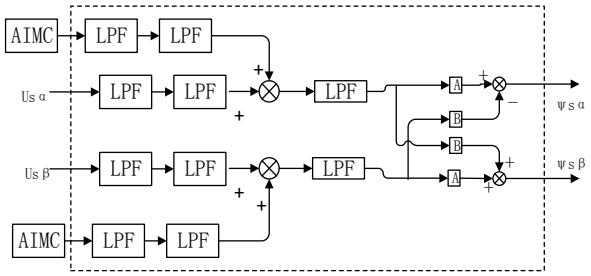

Figure 3: The voltage model with cascaded LPF and the compensation structure

The cut-off angular frequency were defined as $\omega_1, \omega_2, \omega_3$ respectively, compensation amount were defined as X_1, X_2, X_3 respectively, we can obtain:

$$\frac{1}{s+\omega_1} X_1 = \frac{1}{s} \Rightarrow X_1 = 1 - j\frac{\omega_1}{\omega_e}$$

$$\frac{1}{s+\omega_2} X_2 = 1 \Rightarrow X_2 = \omega_2 + j\omega_e$$

$$\frac{1}{s+\omega_3} X_3 = 1 \Rightarrow X_3 = \omega_3 + j\omega_e$$

The total compensation amount: $X = X_1 X_2 X_3$

And $\psi_{s\alpha} + j\psi_{s\beta} = (\psi^*_{s\alpha} + j\psi^*_{s\beta})X$

We can obtain:

$$\begin{cases} \psi_{s\alpha} = A\psi^*_{s\alpha} - B\psi^*_{s\beta} \\ \psi_{s\beta} = B\psi^*_{s\alpha} + A\psi^*_{s\beta} \end{cases} \quad (11)$$

Where:

$$A = \omega_1\omega_2 + \omega_1\omega_3 + \omega_2\omega_3 - \omega_e^2$$

$$B = \omega_2\omega_e + \omega_3\omega_e + \omega_1\omega_e - \frac{\omega_1\omega_2\omega_3}{\omega_e}$$

Connect two LPFs in series after the voltage and current, and in series a LPF in the main circuit, the voltage and current are processed respectively, only need to satisfy that the error of amplitude and phase caused by LPF is the same, cut-off angular frequency can be different, the relationship of cut-off angular frequency is determined by formula (12). Define ω_{i1}, ω_{i2} as the cut-off angular frequency of LPF behind the current respectively, and compensation needed were X_{i1}, X_{i2} respectively, define ω_{u1}, ω_{u2} as the cut-off angular frequency of the two LPFs behind the voltage respectively, the compensation needed were defined as X_{u1}, X_{u2} respectively.

$$X_{i1}X_{i2} = X_{u1}X_{u2} \Rightarrow \begin{cases} \omega_{i1}\omega_{i2} = \omega_{u1}\omega_{u2} \\ \omega_{i1} + \omega_{i2} = \omega_{u1} + \omega_{u2} \end{cases} \quad (12)$$

So can we process the voltage and current respectively.

SIMULATION AND EXPERIMENTAL RESEARCH

In this paper, we simulated and verified in the 2500kw AC-DC-AC synchronous motor vector control system, the synchronous motor is based on the air gap flux-oriented vector control, rated power is 2500KW, rated voltage is 1650V, rated current is 980A, rated frequency is 6.67HZ, stator resistance is 0.0244Ω, stator leakage inductance is 2.52mH, number of pole-pairs is 4. This experiment was built under the PSIM9.0 simulation platform. PSIM9.0 is a professional simulation software used in power electronics and motor control field, its semiconductor switching device is an ideal switch model, and it uses efficient algorithm to overcome the problem that the simulate time is too long, greatly reduced design cycle.

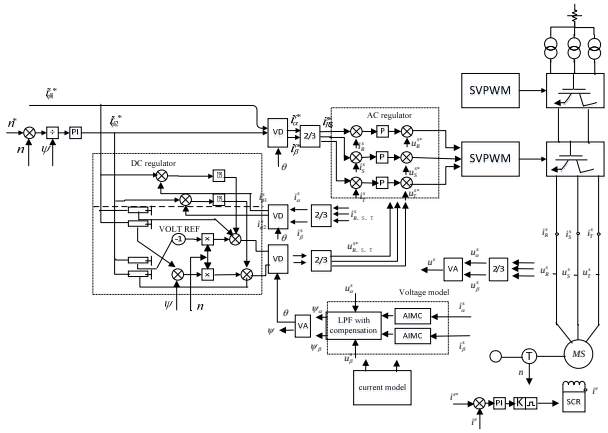

Figure 4: The structure of the large capacity synchronous with AC-DC-AC variable frequency vector control

In Figure 5, the given speed is 100r/min, stator resistance R_s and stator leakage inductance L_{sl} remain the same, after joined the interference D(s)=100V in the 2s, joined the load F=50000N during 2.5-3.5s, we know from original voltage model and the AIMC-based voltage model system flux waveform comparison chart, after joined the disturbance in the 2s, the flux waveforms of original voltage model shifted about 10%, after joined the load in the 2.5s, the flux waveforms shifted about 14%, phase shifted about 12.6 degree, after the rejection of load in the 3.5s, flux waveform shifted smaller, about 10%, but the phase shift still exists. In the 2s, after joined the disturbance, the flux waveform of the voltage model based on AIMC, only shifted about 0.5%, after joined the load, flux waveform shifted about 1%, after the rejection of load in the 3.5s, flux waveform shifted smaller, about 0.5%, and then gradually return to the original stable value. Compared with the two flux waveforms, we see that flux generated by applying the new voltage model structure in the simulation system, shifted smaller in the case of disturbance, and was able to return to a stable state quickly, has a good effect on suppressing and eliminating interference.

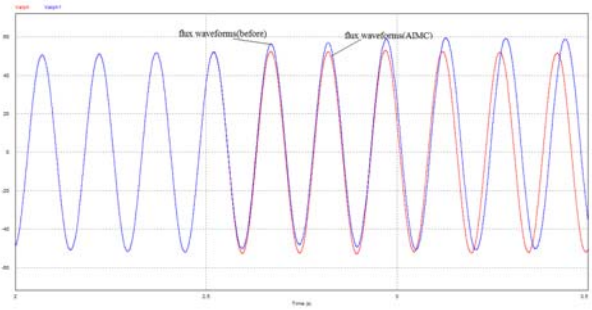

Figure 5: When $R_s = R_s, L_{sl} = L_{sl}, D(s) = 100\text{V}$, the comparison of the simulation flux ($\psi_{s\alpha}$) waveforms

In Figure 6, the given speed is 100r/min, without any disturbance, stator resistance R_s remains the same, in the 2s, make stator leakage inductance $L_{sl}' = 10L_{sl}$, joined the load F=50000N during 2.5-3.5s, we know from original voltage model and the AIMC-based voltage model system flux waveform comparison chart, in the 2s, stator leakage inductance become $L_{sl}' = 10L_{sl}$, the flux waveforms of original voltage model shifted about 4%, and flux waveforms become not smooth, after joined the load in the 2.5s, the flux waveforms shifted about 8%, after the rejection of load in the 3.5s, flux

waveform shifted smaller, about 3%. In the 2s, after stator leakage inductance become $L_{sl}'=10L_{sl}$, the flux waveform of the voltage model based on AIMC only shifted about 0.7%, after joined the load, flux waveform shifted about 1%, after the rejection of load in the 3.5s, flux waveform shifted smaller, about 0.6%, and then gradually return to the original stable value, flux waveforms keep smoothly. Compared with the two flux waveforms, we see that flux generated by applying the new voltage model structure in the simulation system, shifted smaller when stator leakage inductance changes, and returned to a stable state quickly, has a better stability on the stator winding leakage inductance parameter variation.

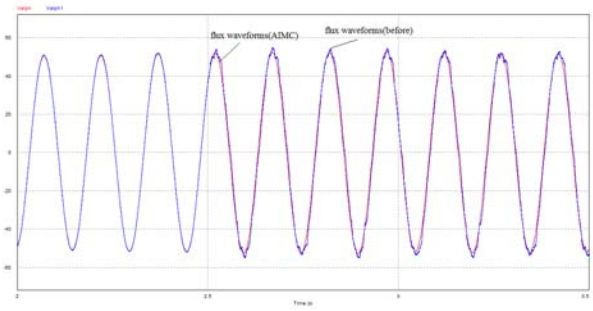

Figure 6: When $R_s=R_s, L_{sl}=10L_{sl}, D(s)=0\text{V}$, the comparison of the simulation flux($\psi_{s\alpha}$) waveforms

In Figure 7, the given speed is 100r/min, without any disturbance, stator leakage inductance L_{sl} remains the same, in the 2s, make stator inductance $R_s'=1000R_s$, joined the load F=50000N during 2.5-3.5s, we know from original voltage model and the AIMC-based voltage model system flux waveform comparison chart, in the 2s, stator leakage inductance become $L_{sl}'=10L_{sl}$, the flux waveforms of original voltage model shifted about 8%, after joined the load in the 2.5s, the flux waveforms shifted about 12%, after the rejection of load in the 3.5s, flux waveform shifted smaller, about 3%. After stator leakage inductance become $L_{sl}'=10L_{sl}$ in the 2s, the flux waveform of the voltage model based on AIMC only shifted about 0.5%, after joined the load, flux waveform shifted about 1%, after the rejection of load in the 3.5s, flux waveform shifted smaller, about 0.4%, and then gradually return to the original stable value. Compared with the two flux waveforms, we see that flux generated by applying the new voltage model structure in the simulation system, shifted smaller when stator inductance changes, and returned to a stable state quickly, has a better stability on the stator resistance parameter variation.

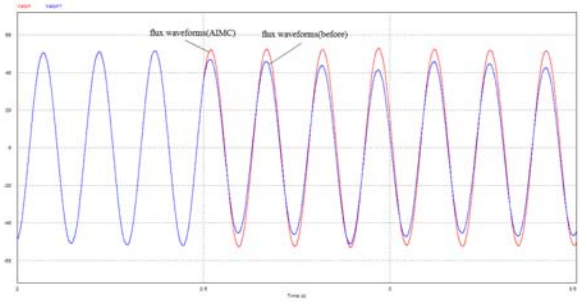

Figure 7: When $R_s=1000R_s, L_{sl}=L_{sl}, D(s)=0\text{V}$,the comparison of the simulation flux($\psi_{s\alpha}$) waveforms

In Figure 8, the given speed is 100r/min, no-load stable operation, the flux waveform and flux circle are as follows. When there is no disturbance and the parameters remain the same, the flux waveform is smooth, the flux circle has a good effect.

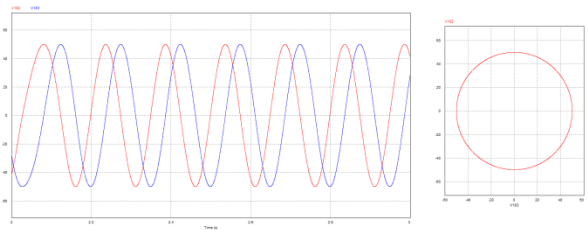

Figure 8: The simulation flux($\psi_{s\alpha}$, $\psi_{s\beta}$) waveforms

CONCLUSIONS

In this paper, we combined adaptive control with internal model control technology, for large capacity synchronous motor vector control system, we built voltage model flux observer of the adaptive internal control model, aimed at large capacity synchronous motor vector control system, theoretical analysis and simulation results show that:

1).The voltage model flux observer of the adaptive internal control model, for stator inductance and stator leakage inductance parameters variation, has good dynamic performance and robustness.

2).Considering the disturbance canceling structure in the adaptive control system, has a good effect on eliminate disturbance.

3).Cascaded LPF and the compensation structure improved the integral saturation caused by the pure integral element.

ACKNOWLEDGEMENT

This work is supported by National Natural Science Foundation of China (Normal Project No. 61170115), (Key Proj ect No.61432004) and National Key Technologies R&D Program of China (No.2014BAF08B04). This work was supported by the Foundation of Beijing Engineering and Technology Center for Convergence Networks and Ubiquitous Services.

RERERENCES

[1] Q.B. Jin, Q. Liu. Analytical IMC-PID design in terms of performance/ robustness tradeoff for integrating processes: From 2-Dof to 1-Dof. Journal of Process Control,2014,24: 22-32.

[2] Zhao Zhicheng,Liu Zhiyuan, Xia Zhimin, et al. Internal Model Control Based on LS-SVM for a Class of Nonlinear Process. Physics Procedia, 2012,25: 1900-1908.

[3] Zhu Hairong, Li Qi, Gu Juping,et al. Adaptive internal model control of a test turntable based on inertia identification. Control Theory & Applications, 2013, 30(2):201-207(in Chinese).

[4] Riccardo Marino, Patrizio Tomei. Disturbance cancellation for linear systems by adaptive internal models. Automatica,2013,49:1494-1500.

[5] Song Wenxiang. Yin Yun. A Control Strategy of Three-Phase PWM Rectifier Based on Internal Model Control. Transactions Of China Electrotechnical Society, 2012,27(12):94-101(in Chinese).

[6] Micky Rakotondrabe,et al. Control of a Novel 2-DoF MEMS Nanopositioner With Electrothermal Actuation and Sensing. IEEE Transactions On Control Systems Technology, 2014, 22(4):1486-1497.

[7] N. Amuthan, P. Subburaj, P. Melba Mary. Direct model reference adaptive internal model controller for better voltage sag ride through in doubly fed induction generator wind farms. Electrical Power and Energy Systems,2013,47:255-263.

[8] Zhou Ying, Nie Panpan, Liu Zhigang,et al. An application research of adaptive fuzzy internal model control in the fermentation system. Journal Of Hebei University Of Technology, 2012,41(5):10-14(in Chinese).

[9] Shen Gang, Zhu Zhencai,Zhang Lei.et al. Adaptive feed-forward compensation for hybrid control with acceleration time waveform replication on electro- hydraulic shaking table. Control Engineering Practice, 2013, 21:1128-1142.

[10] Wang Qian, Li Xinguo. Adaptive Inverse Control of a Generic Hypersonic Vehicle Based on Improved EMRAN. Procedia Engineering,2011,15:277-281.

[11] Zhou Yangzhong,Xu Haijun.Nonlinear Internal Model Control for Permanent Magnet Synchronous Generating Systems.Proceedings of the CSEE, 2013, 33(6):128-135(in Chinese).

[12] Q.B. Jin, Q. Liu. IMC-PID design based on model matching approach and closed-loop shaping. ISA Transactions, 2014,53:462-473.

[13] John Porrill, Paul Dean, Sean R. Anderson. Adaptive filters and internal models: Multilevel description of cerebellar Function. Neural Networks,2013,47:134-149.

[14] N. Amuthan, P. Subburaj, P. Melba Mary. Voltage sag ride through using Improved Adaptive Internal Model Controller for doubly fed induction generator wind farms. Computers and Electrical Engineering,2013,39:214-224.

[15] Chen Zenglu, Ma Xin, Ji Hongyang,et al. A Novel Drift-estimated and Feedback- corrective Algorithm for Voltage Model of Stator Flux. Proceedings of the CSEE, 2014, 34(18): 3035-3041 (in Chinese).

[16] Chang Qiankun, Ge Qiongxuan, Zhang Bo. Research on the Band-Pass-Filter Compensation Voltage Model of Induction Motors. Proceedings of the CSEE, 2014, 34(9):1404-1414(in Chinese).